

Article

Cite this article: Lopezalles, S. M. (2025). Leveraging functional morphology to increase accuracy of body-mass estimation: a study using canids. *Paleobiology*, 1–13. <https://doi.org/10.1017/pab.2025.1>

Received: 27 April 2024
Revised: 12 December 2024
Accepted: 02 January 2025

Handling Editor:
Matthew McCurry

Corresponding author:
Sierra M. Lopezalles;
Email: slopezal@iu.edu

Leveraging functional morphology to increase accuracy of body-mass estimation: a study using canids

Sierra M. Lopezalles 

Department of Biology, Indiana University, Bloomington, Indiana 47405, U.S.A.

Abstract

Body mass is an important facet of reconstructing the paleobiology of fossil species and has, historically, been estimated from individual skeletal measurements. This paper demonstrates the potential advantages of estimating body mass using 3D geometric morphometrics on limb bones, which allows size to be explicitly contextualized within the functional morphology of the animal. Geometric morphometrics of the humerus and femur is used to estimate body mass in domestic dogs and wild canids, and the resulting estimates are compared with estimates made using limb bone dimensions and centroid size. In both groups, 3D methods produced more accurate estimates of body mass than linear dimensions. Additionally, centroid size was a poor predictor of body mass and should not be preferred over linear measurements. The use of 3D methods also reveals specific aspects of shape that are associated with different sizes. In general, relatively heavier individuals were associated with more robust bones and wider articulation sites, as well as larger attachment sites for muscles related to flexion and extension of the shoulder and hip joints. The body-mass equations constructed based on dogs were further evaluated on wild canids, as a test of their potential efficacy on fossil canids. With some adjustments, the body-mass estimation equations made for domestic dogs were able to reliably predict the mass of wild canids. These equations were then used to estimate body mass for a selection of fossil canids: *Canis latrans*, 16 kg; *Aenocyon dirus*, 67 kg; *Phlaocyon multicuspus*, 8 kg; and *Hesperocyon gregarius*, 2.5 kg.

Non-technical Summary

Estimates of body mass for extinct species are an important part of paleobiological reconstruction, as size influences many aspects of ecology and physiology. Historically, body mass has been estimated from linear regressions on skeletal measurements. This paper demonstrates the potential advantages of estimating body mass using the 3D shape of the limb bones instead of individual measurements. The shape of the humerus and femur are used to estimate body mass in domestic dogs and wild canids, and the resulting estimates are compared with estimates made using skeletal dimensions. In both groups, 3D methods produced more accurate estimates of body mass than linear dimensions. The use of 3D methods also reveals specific aspects of shape that are associated with different sizes. In general, relatively heavier individuals were associated with overall more robust bones, with wider articulation sites, as well as larger attachment sites for muscles related to flexion and extension of the shoulder and hip joints. The body-mass equations constructed based on domestic dogs were further evaluated on wild canids, as a test of their potential efficacy on fossil canids. With some adjustments, the body-mass estimation equations made for domestic dogs were able to reliably predict the mass of wild canids. These equations were then used to make estimates of body mass for a selection of fossil canids: *Canis latrans*, 16 kg; *Aenocyon dirus*, 67 kg; *Phlaocyon multicuspus*, 8 kg; and *Hesperocyon gregarius*, 2.5 kg.

Introduction

Body size is one of the most important variables for paleobiological reconstruction. Body size is highly correlated with most physiological and life-history characteristics; hence, determining the size of a fossil organism can lead to a suite of other conclusions about its ecology. In particular, body size in mammals is correlated with metabolic rate; life span; rate of development; reproductive behavior; niche partitioning; and numerous other morphological, behavioral, physiological, and ecological factors (Eisenberg 1981; McNab 1990 and references therein). For carnivores, body size also plays an important role in predation strategies. Terrestrial carnivores larger than 21.5 kg dominantly hunt large prey items (their size or larger), while predators below that threshold feed on small prey due to mass-related energy requirements (Carbone et al. 1999). In wolves, higher body mass is also associated with better predatory performance (MacNulty et al. 2009). Thus, estimating body size is often the first step toward reconstructing the ecology of fossil organisms.

© The Author(s), 2025. Published by Cambridge University Press on behalf of Paleontological Society. This is an Open Access article, distributed under the terms of the Creative Commons Attribution-NonCommercial-ShareAlike licence (<http://creativecommons.org/licenses/by-nc-sa/4.0>), which permits non-commercial re-use, distribution, and reproduction in any medium, provided the same Creative Commons licence is used to distribute the re-used or adapted article and the original article is properly cited. The written permission of Cambridge University Press must be obtained prior to any commercial use.

PALEOBIOLOGY
A PUBLICATION OF THE
 PALEONTOLOGICAL SOCIETY

 **CAMBRIDGE**
UNIVERSITY PRESS

Historically, many methods have been applied to this problem. These methods can be divided into two broad categories: volumetric density estimation in the fossils themselves and scaling of skeletal variables from extant taxa. This study will focus on extant-scaling methods, although volumetric methods, such as minimum convex hull and volumetric model estimation, are also becoming more accurate with improvements in technology (Rovinsky et al. 2020).

The majority of extant-scaling equations have been constructed by: (1) choosing a measurement or set of measurements that are assumed to covary with body size, (2) constructing a dataset of living animals of known body mass that are expected to be representative based on phylogenetic relation or functional similarity, and (3) regressing body mass onto the selected measurement and using the resulting equation for future predictions (Van Valkenburgh 1990; Anyonge 1993; Egi 2001; Ruff 2003; Losey et al. 2015, 2017).

Extant-scaling equations for body-mass estimation are often split between cranial and postcranial metrics. While cranial and dental elements are taxonomically diagnostic and frequently recovered in the fossil record, it has been repeatedly shown that estimations based on postcranial measurements are more reliable and provide a higher degree of accuracy (Van Valkenburgh 1990; Egi 2001). In contrast to cranio-dental measurements, postcranial elements like limb bones must directly transmit and withstand the weight of the body and thus should have a tighter correlation with body mass.

Across the order Carnivora, many equations for estimating body mass have been constructed based on a variety of different metrics, including cranio-dental measurements (Van Valkenburgh 1990), limb bone articular and cross-sectional dimensions (Anyonge 1993; Egi 2001), articular circumference (Andersson 2004), and centroid sizes obtained from 3D analysis of the mandible and the elbow (Meloro and O'Higgins 2011; Figueirido et al. 2015).

These methods are based on the simple expectation that larger animals have larger bones and teeth, with the assumption that the size of these structures will scale consistently with overall size across a clade with some transformation or the other (e.g., log scale). While generally accurate, this method assumes that the data can be transformed to have an approximately linear relationship and has historically been confined to using only a few measurements as the basis for extrapolating body mass. Yet mammals do not compensate for increased size only by increasing the size or robustness of their bones; other mechanisms can be leveraged to manage changes in body mass. These methods, including shifts in posture to place the limbs more in line with ground reaction forces (Biewener 1989), may not be reflected by changes in simple measurements of cross-sectional area or articular dimensions. The complicated nature of this problem requires a complex solution that can integrate aspects of size with those of shape, including patterns of muscle attachments, curvature, and articular structure—such as that which can be constructed using 3D geometric morphometrics. However, while 3D landmark methods have become prevalent in studies of functional morphology, they have yet to be fully applied to the subject of body-mass estimation.

The main way that geometric morphometrics has been applied to the question of body-mass estimation is by using the centroid size of an element as a proxy for body size. When geometric morphometric methods are applied, generalized Procrustes analysis (GPA) is used to align landmarked samples by centering them on the centroid, then rotating and scaling each specimen while minimizing the sum of squared distances between corresponding landmarks

(Rohlf and Slice 1990). Through the rescaling of each specimen, the aspects of size and shape are separated, with the intention of allowing shape to be analyzed free from the influence of size. Size variation is instead captured by the centroid size, computed as the square root of the sum of the squared distances of all landmarks from their centroid. Thus, centroid size has been employed as a proxy for overall size and used to construct body-mass estimation equations for a variety of clades (Hood 2000; Meloro and O'Higgins 2011; Cassini et al. 2012; Figueirido et al. 2015).

Geometric morphometric data are often considered “size-free,” because each object has been rescaled to centroid size; however, important correlates of size are still found in the rescaled coordinates because of the allometry between body size and shape. Size allometry is well known in geometric morphometric studies, and even after GPA, the first component of principal components analysis (PCA) is still often strongly associated with size (Martín-Serra et al. 2014a) (more generally, there still remains a significant relationship between body mass and shape; Meloro and O'Higgins 2011). Thus, estimation equations based solely on centroid size fail to consider the aspects of shape that are independent of mathematical scaling.

In particular, features related not only to the size of bones but their efficiency in supporting weight may have an allometric relationship with size. The size and placement of muscle attachments, as well as the shape of articulation areas determine how weight is transmitted through the skeleton and are expected to covary with body mass. Three-dimensional landmarking methods, like the one described here, intentionally incorporate shape features that might have an allometric relationship with size into the model in order to improve their estimates.

While 3D landmarking can be more complicated and time-intensive than simple linear measurements, it captures much more variation in form that can be leveraged for higher accuracy. Furthermore, any study that already uses centroid size requires an equal degree of effort in creating and placing the 3D landmarks but ignores the added information captured by integrating shape into the estimation.

Three-dimensional geometric morphometric methods capitalize on all aspects of shape, including articular dimensions, the size of muscle attachments, and the robustness of the bone, while still retaining the aspect of raw size. This may lead to estimates of body mass that are both more accurate and explicitly contextualize size within the functional interpretation of the animal. The primary goal of this study is to demonstrate the utility of geometric morphometrics for body-mass estimation. Secondarily, it tests the efficacy of using regressions constructed on domestic dogs to estimate body mass in extant wild canids and fossil canids.

Methods

Materials

This study uses 3D geometric morphometrics of the stylopod limb bones (humerus and femur) to estimate body mass. The dataset included full-body computed tomography (CT) scans for 61 adult domestic dogs from the University of Missouri at Columbia Veterinary Health Center. Scans were selected randomly from the veterinary database after confirming that they had a recorded breed and that the scan contained both the humerus and the femur. The majority of scans were of living dogs that were scanned for medical reasons, although a small subset of scans were postmortem. All scans were scanned on the Toshiba Aquilion ONE medial CT scanner with a resolution of 0.64 mm² and a slice thickness of 2 mm.

The dataset includes representatives from 35 different breeds recognized by the American Kennel Club (AKC 2023), spanning the range of dog sizes from the Chihuahua (2 kg) to the Newfoundland (63 kg) (Fig. 1, Supplementary Table 1, Supplementary Fig. 1). Notably, the accompanying metadata associated with veterinary scans includes the dog's weight at the time of the scan, which avoids the loss of precision associated with using breed average weights. The humerus ($n = 56$) and femur ($n = 51$) of each specimen were segmented out in 3D Slicer (Fedorov et al. 2012). Elements from the right side were preferentially used. If the right limb bone was unavailable for any reason (e.g., broken, obscured on CT scan), then the left was used and mirrored.

A second dataset of 43 wild canid specimens was obtained from MorphoSource or digitized using structured light surface scanning and photogrammetry (Supplementary Table 2). This dataset included representatives from 21 different species and contained 43 humeri and 34 femora. All of the specimens were housed in the institutions listed in the following section. All wild canid specimens used are archived and available on MorphoSource. Average body mass for each species was estimated from the literature as the midpoint of published mass ranges (Supplementary Table 2). If there were separate estimates for each sex, then the average of the midpoints was used.

Institutional Abbreviations. AMNH: American Museum of Natural History, New York, NY; ARCVES: Arizona Research Collection for Integrative Vertebrate Education and Study, Glendale, AZ; DMU: Des Moines University, Des Moines, IA; FMNH: Field Museum of Natural History, Chicago, IL; FLMNH: Florida Museum of Natural History, Gainesville, FL; IMNH: Idaho Museum of Natural History, Pocatello, ID; USNM: National Museum of Natural History, Washington, D.C.; UMZC: University Museum of Zoology, Cambridge, U.K.; WRAZL: Williams R. Adams Zooarchaeology Laboratory, Bloomington, IN.

Three-Dimensional Landmarks. A set of homologous landmarks were applied to each limb bone to capture the full shape of the bone using 3D Slicer (Fig. 2A, Supplementary Table 4). Landmark points were chosen to capture the range of morphological variation across dog breeds, focusing on locations of important muscle attachments (see Fig. 2B,C). Humerus landmarks were based partially on Fabre et al. (2014) and Martín-Serra et al. (2014a) with modifications. Femur landmarks included the landmarks used by Martín-Serra et al. (2014b), with additional landmarks

added to encompass more detail in the shape of the greater trochanter and trochlea.

Procrustes superimposition and PCA were performed on the landmark points using the geomorph package in R (R Core Team 2018; Adams et al. 2021). The centroid size for each specimen was measured as the square root of the sum of the squared distances of all landmarks from their centroid. PCA was performed separately for wild canids and domestic dogs. To estimate wild canid body mass using the domestic dog equations, the wild canid specimens were rotated into the dog PCA space after it was constructed.

Estimating Percent Measurement Error. Landmarking error was measured using the “new old method for assessing measurement error” (Bailey and Byrnes 1990). This method uses model II analyses of variance and covariance to compare within-group variance and between-group variance, where groups represent multiple landmarking attempts on the same specimen. Measurement error is calculated as:

$$\%ME = \frac{\text{within-group variance}}{\text{within-group variance} + \text{between-group variance}} * 100 \quad (1)$$

where within-group variance is the variance between landmarking attempts on the same specimen and between-group variance is:

$$\text{Between-group variance} = \frac{\text{within-group variance} + \text{mean squares between}}{2 \text{ measurements per specimen}} * 100 \quad (2)$$

For both limb bones, each specimen was landmarked twice, and error was computed between these replicates.

Linear Measurements. As a point of comparison for the 3D prediction equations, three element dimensions were measured on each specimen. Dimensions were chosen based on the prediction equations with the lowest percent prediction error and highest R^2 values from Losey et al. (2017). This was proximal depth and distal breadth for the humerus and proximal head breadth and total proximal breadth for the femur. In addition, greatest length was measured for both limb bones as a point of reference, although it is known to be a poor estimator of body size (Egi 2001). See Supplementary Figure 2 for illustrations of the linear measurements, following Von den Driesch (1976) and Losey et al. (2017).

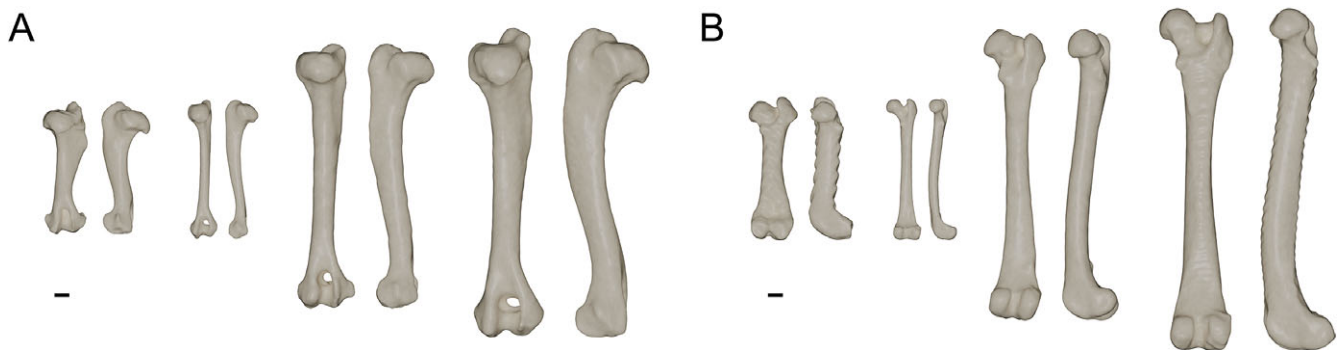


Figure 1. Proximal limb bone variation across domestic dog breeds. **A**, Humerus shape in four different breeds. For each pair of humeri, posterior view is on the left and medial view is on the right. **B**, Femur shape in four different breeds. For each pair of femora, posterior view is on the left and medial view is on the right. For both humeri and femur, dogs breeds from left to right are Jack Russell terrier, Pomeranian, golden retriever, Great Pyrenees. Scale bar, 1 cm. Geometric staggering of the shaft in the Jack Russell terrier is an artifact of segmenting the computed tomography (CT) scan.

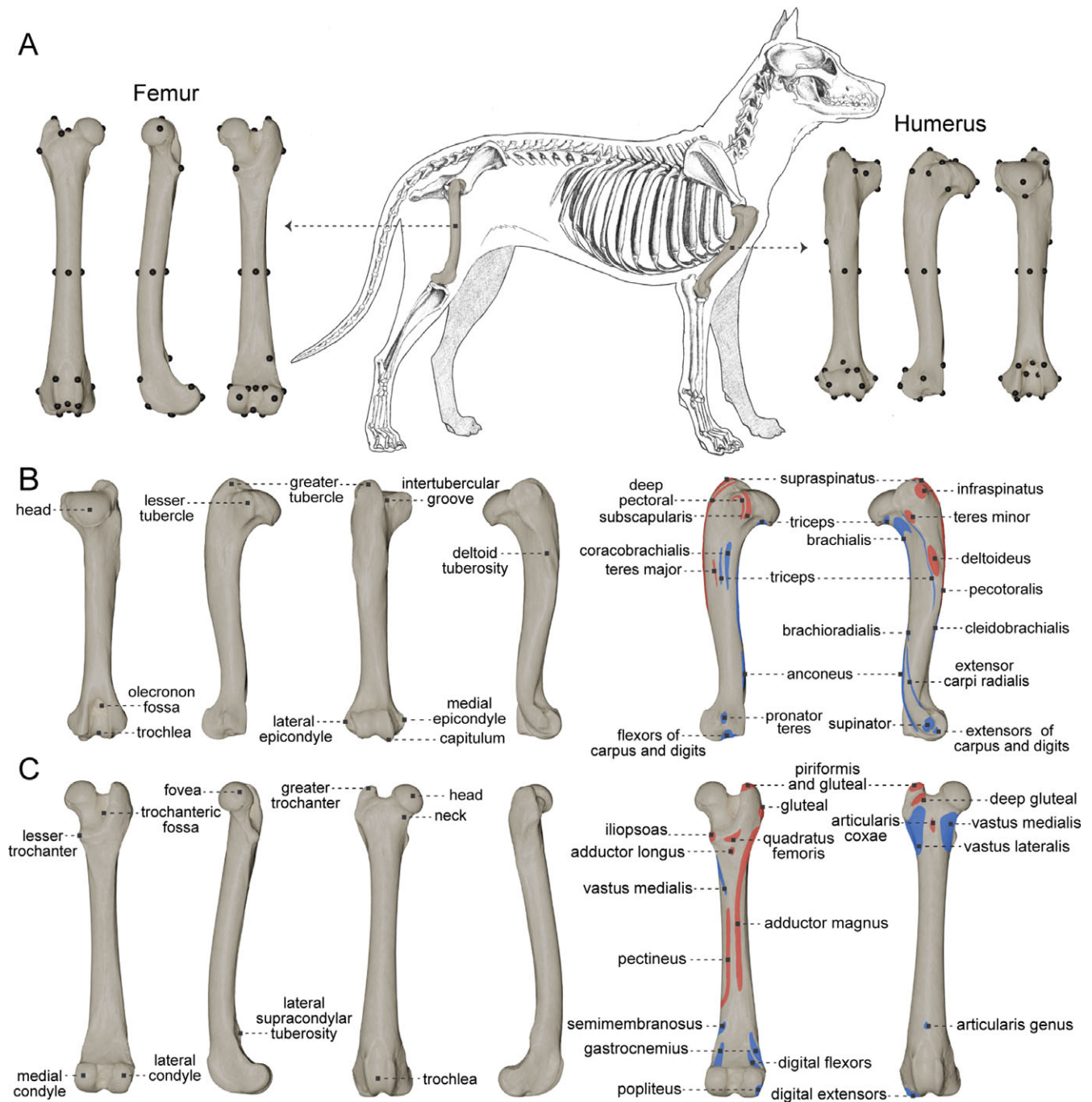


Figure 2. Orientation to the dog skeleton and the bones used in this analysis. **A**, Humerus and femur, exemplified on a domestic dog and demonstration of the landmarks used. The humerus model represents mean shape across the domestic dog dataset. Humerus views are anterior, medial, then posterior. An English bulldog was used for the femur model, which is close to mean shape. Femur views are anterior, medial, posterior. One femoral landmark is hidden from view at the deepest point in the trochanteric fossa. **B**, Key morphological features of the humerus. From left to right: posterior view, medial view, anterior view, lateral view. **C**, Key morphological features of the femur. From left to right: posterior view, anterior view, medial view, lateral view. Major muscle origins (red) and insertions (blue) are shown. Note that many of the muscles depicted do not leave visible markers that can be landmarked and therefore are not discussed further. Anatomical features referenced from Evans and Miller (1993).

Regressions

A series of ordinary least squares linear regressions of log body mass onto various predictor variables were computed and compared. Body mass, centroid size, and all linear measurements were natural log transformed, because body mass has cubic growth, while centroid size and element dimensions grow linearly. Log mass was regressed against log centroid size and selected principal components (PCs) in order to obtain equations for estimating body mass

in domestic dogs and wild canids. For comparison, additional regressions of log mass against individual linear measurements and centroid size alone were also computed.

PCs were selected by best subset regression using the *olsrr* package in R (Hebbali 2024). Only the first 10 PCs were considered, as higher PCs capture much less variance, and potential models were compared based on their Bayesian information criterion (BIC). BIC is a model comparison method that estimates the log-

likelihood fit of a model while penalizing for large numbers of estimating parameters. It was chosen for its strictness, which effectively limited the size of the models to avoid overfitting.

For each regression, R and R^2 values, % prediction error (%PE), and % standard error of the estimate (%SEE) are reported.

The %PE is calculated as:

$$\%PE = \frac{\text{observed body mass} - \text{predicted body mass}}{\text{predicted body mass}} * 100 \quad (3)$$

Similarly, SEE is calculated as the root-mean-square error, and the %SEE is:

$$\%SEE = \frac{SEE}{\text{mean observed body mass}} * 100 \quad (4)$$

based on Van Valkenburgh (1990).

The delta Akaike information criterion (ΔAIC) was used to compare regressions across each skeletal element. AIC is similar to BIC but has a slightly lower penalty for additional parameters. ΔAIC is the difference in score between the best model and all other models; by nature, this sets the ΔAIC for the best model to zero. AIC comparisons between regressions were calculated using the AICc-modavg package in R (Mazerolle 2023).

Following the creation of body-mass estimation equations for domestic dogs, these equations were used to estimate body mass in wild canids.

Fossil Specimens

To demonstrate the applicability of this method, the body mass of four fossil canids was estimated (Supplementary Table 3). Fossil specimens included seven specimens of *Aenocyon dirus*, two specimens of *Hesperocyon gregarius*, two specimens of *Canis latrans orcutti*, and a single specimen of *Phlaocyon* (presumed *P. multicuspus* based on locality and size) from the Field Museum of Natural History and the Natural History Museum of Los Angeles County. All specimens were surface scanned using the Creafom Go!Scan 20 at a resolution of 0.3 mm, except LACM PMS9555, which was downloaded from MorphoSource. These specimens were landmarked in 3D Slicer and rotated into both the domestic dog and wild canid PCA space for body-mass estimation.

Results

Landmarking Error

The degree of landmarking error for both bones was low (in comparison to measurement error in other studies, which ranged from <1% to 100%; Yezerinac et al. 1992; Muñoz-Muñoz and Perpiñán 2010), although higher in the humerus (12%) compared with the femur (4%). These results were based on comparing landmark placement between two replicates for each domestic dog humerus and femur. For the humerus, 5% of the error is driven by the four landmarks capturing the center of the shaft, likely due to the difficulty in consistently determining the midpoint of the shaft.

Element Dimensions

The regressions of log body mass onto the six limb bone measurements yielded a range of correlation coefficients from 0.88 to 0.93 in domestic dogs (Table 1) and 0.83 to 0.91 in wild canids (Table 2).

In dogs, percent prediction errors (%PE) ranged from 19–25% and percent standard error of the estimate (%SEE) from 20–36% for the three measurements. Error levels and correlation coefficients

Table 1. Statistics for linear regression equations for domestic dog body mass. Sample sizes for the groups: humerus, 56; femur, 51. The best regression based on ΔAIC for each limb bone is bolded. PCs are visualized in Fig. 3 for the humerus and Fig. 4 for the femur. Abbreviations: %PE, percent prediction error; %SEE, percent standard error of the estimate; ΔAIC , delta Akaike information criterion; PC, principal component

Regression equation	R	R^2	%PE	%SEE	ΔAIC
Humerus					
Log humerus length	0.939	0.881	24.12	25.22	39.69
Log distal humerus breadth	0.957	0.916	21.00	28.42	20.35
Log proximal humerus depth	0.959	0.919	19.90	26.81	18.13
Log centroid size	0.928	0.862	26.07	25.75	48.02
Log centroid size + PC 1	0.964	0.929	18.85	25.79	13.24
Log centroid size + PCs 1, 2, 9	0.974	0.949	16.19	21.67	0.0
Femur					
Log femur length	0.941	0.886	24.16	23.15	28.77
Log femoral head breadth	0.940	0.884	24.96	36.48	29.79
Log proximal femur breadth	0.965	0.931	18.79	20.01	2.88
Log centroid size	0.937	0.878	25.18	23.61	32.13
Log centroid size + PC 1	0.963	0.928	18.56	22.72	7.64
Log centroid size + PCs 1, 3, 7	0.972	0.944	16.59	21.66	0.0

were comparable for the humerus and the femur. For the humerus, proximal humerus depth (%PE = 20, %SEE = 27) was the best predictor of body mass, while proximal femur breadth (%PE = 19, %SEE = 20) was the best predictor for the femur. Greatest length was a poor predictor of body mass for both limb bones, however femoral head breadth (%PE = 25, %SEE = 36) had even lower correlations and higher error.

Similar patterns were seen in the wild canids, although with overall higher error levels: %PE ranged from 19–26% and %SEE from 31–49%. For both limb bones, greatest length was the worst predictor (as determined by AIC), while proximal humerus depth (%PE = 19, %SEE = 31) was the best predictor for the humerus and femoral head breadth (%PE = 27, %SEE = 35) was the best predictor for the femur.

Coefficients and intercepts for element dimension regressions can be found in Supplementary Table 5.

Centroid Size

In comparison to limb bone measurements, centroid size is a poor predictor of body mass. For the domestic dogs, centroid size alone was the worst predictor of body mass and had higher %PE and %SEE values than all of the linear measurements in both the humerus (%PE = 26, %SEE = 26) and in the femur (%PE = 25, %SEE = 24). This was also true for the wild canids, where centroid size was again the worst predictor for the humerus (%PE = 28, %SEE = 49) and the femur (%PE = 25, %SEE = 49).

Shape

For both limb bones, across both groups, a combination of centroid size and shape was a better predictor of body mass than any linear measurement. The addition of a single PC to centroid size led to

Table 2. Statistics for linear regression equations for wild canid body mass. Sample sizes for the groups: humerus, 43; femur, 35. The best regression, based on Δ AIC, for each limb bone is bolded. For the dog estimation equations, the best regression was chosen based on %PE. PCs are visualized in Fig. 5. Abbreviations: %PE, percent prediction error; %SEE, percent standard error of the estimate; Δ AIC, delta Akaike information criterion; PC, principal component

Regression equation	R	R^2	%PE	%SEE	Δ AIC
Humerus					
Log humerus length	0.913	0.834	25.90	45.67	30.62
Log distal humerus breadth	0.948	0.899	21.80	33.38	9.30
Log proximal humerus depth	0.953	0.908	19.45	31.01	5.22
Log centroid size	0.904	0.817	28.06	48.85	34.94
Log centroid size + PC 1	0.955	0.912	19.79	28.64	5.69
Log centroid size + PCs 1, 8	0.963	0.928	19.06	23.29	0.0
Dog distal humerus breadth	—	—	23.31	35.72	—
Dog proximal humerus depth	—	—	26.59	47.34	—
Dog shape equation	—	—	69.98	82.35	—
Dog shape equation adjusted	—	—	21.02	36.35	—
Femur					
Log femur length	0.927	0.857	24.65	49.61	11.36
Log femoral head breadth	0.940	0.883	26.57	34.66	4.35
Log proximal femur breadth	0.934	0.872	25.98	33.80	7.37
Log centroid size	0.922	0.850	25.02	49.11	13.04
Log centroid size + PC 1	0.950	0.903	22.27	28.70	0.39
Log centroid size + PCs 1, 3	0.954	0.911	21.94	29.41	0.0
Dog femoral head breadth	—	—	27.98	33.68	—
Dog proximal femur breadth	—	—	43.41	64.31	—
Dog shape equation	—	—	80.44	89.13	—
Dog shape equation adjusted	—	—	23.29	40.76	—

higher R^2 values and lower error than centroid size alone or any single measure of element dimensions. For the humerus in domestic dogs, incorporating one PC alongside centroid size raised the R^2 from 0.86 to 0.93 and lowered the %PE from 26% to 19%. The addition of two more components (PCs 2 and 9) further raised the correlation to 0.95. This combination of centroid size and PCs has the overall lowest error for domestic dogs (%PE = 16, %SEE = 22).

The morphology associated with each PC is visualized in Figure 3. Because the polarity of PCs is arbitrary, all PCs were oriented such that higher scores were associated with heavier masses (relative to centroid size). The first PC is characterized by the continuum from extreme curvature and robustness to gracile bones with comparatively smaller epiphyses and longer and thinner shafts at the other. In this context, robustness is defined as bones that are wide for their length, with comparatively larger epiphyses. Robust bones have higher PC 1 scores, and thus, through the regression, are associated with higher estimates of body mass. Higher scores on PC 2 are associated with comparatively larger

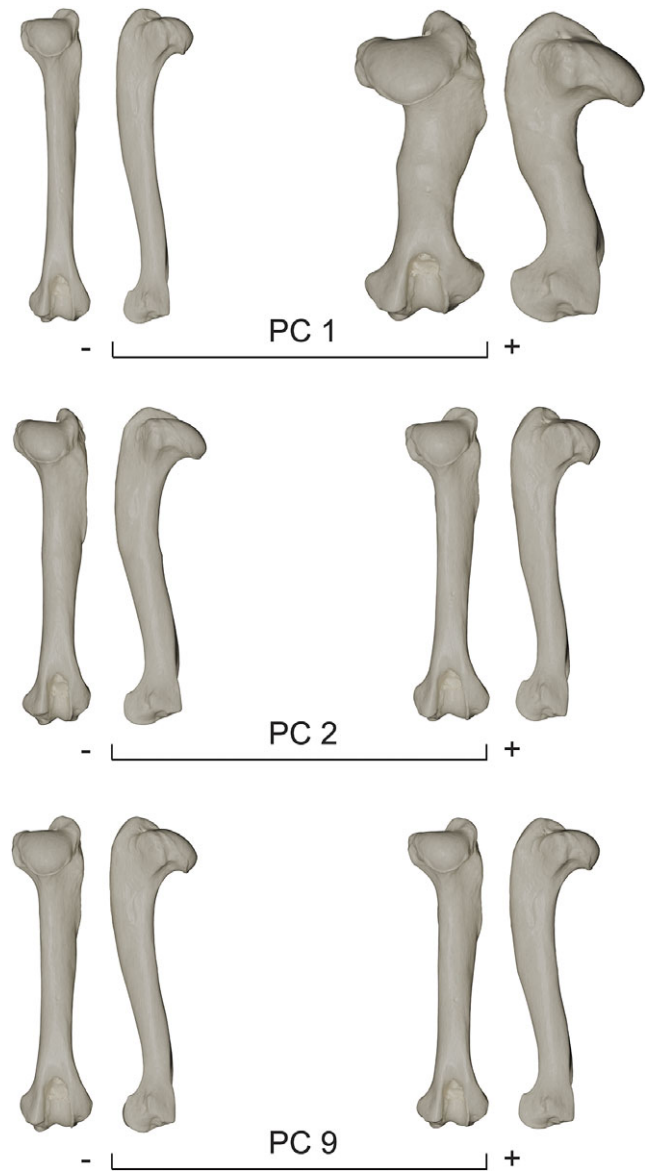


Figure 3. Relevant axes of humeral variation in domestic dogs. Models show the shape changes associated with the minimum and maximum score for each principal component (PC). PCs are oriented such that heavier individuals are associated with positive scores. For each pair of humeri, posterior view is on the left and medial view is on the right.

epiphyses and a reduction in shaft curvature, as well as a larger greater tubercle and a proximally shifted deltoid tuberosity. Similarly, higher scores on PC 9 are also associated with a larger greater tubercle, in addition to a deeper humeral head. Together PCs 1, 2, and 9 comprise 60% of the variance in humerus shape (51%, 7%, and 2%, respectively).

Similar patterns emerge for the domestic dog femur, with a single PC raising the correlation from 0.88 to 0.93, lowering the %PE from 25% to 19%, and lowering the %SEE from 24% to 23%. The additional incorporation of PCs 3 and 7 further increases the correlation to 0.94 and lowers the %PE to 17%.

Similar to the humerus, PC 1 for the femur describes a continuum from gracile to robust (Fig. 4). Higher scores on PC 3 are associated with a larger greater trochanter and shorter femoral necks, while PC 7 describes the size of the lateral supracondylar

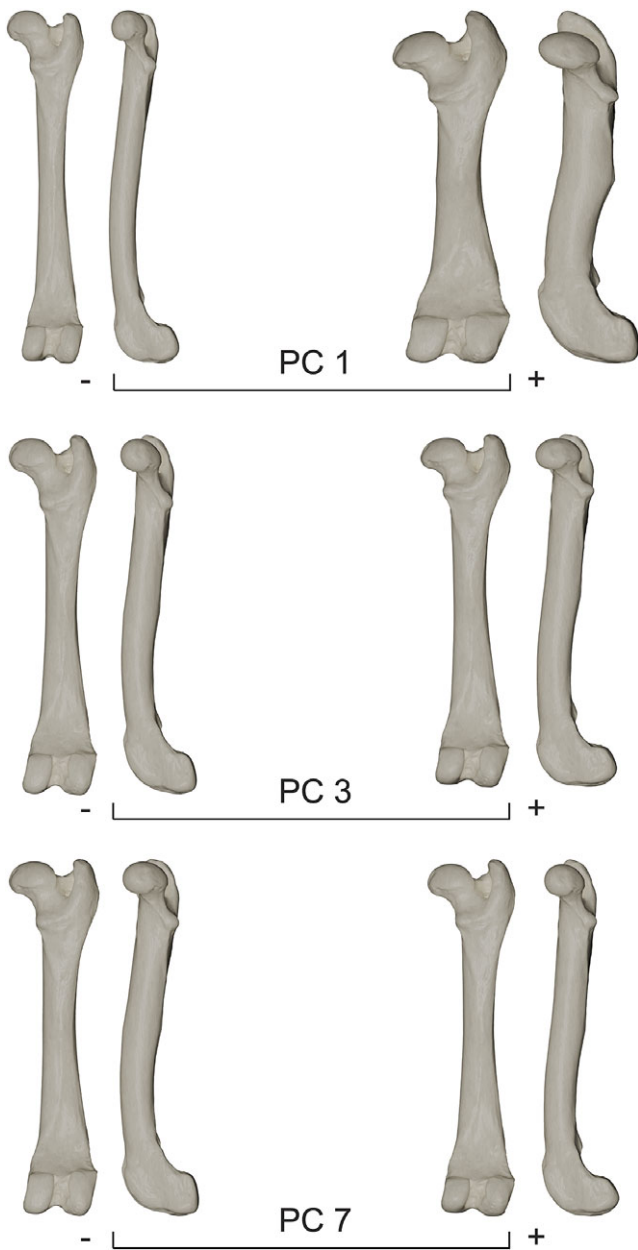


Figure 4. Relevant axes of femoral variation in domestic dogs. Models show the shape changes associated with the minimum and maximum score for each principal component (PC). PCs are oriented such that heavier individuals are associated with positive scores. For each pair of femora, posterior view is on the left and medial view is on the right. The stretched shape of the femoral head is an artifact of the warping process.

tuberosity, with higher scores pointing to a larger tuberosity. PCs 1, 3, and 7 comprise 56% of the variance in femoral shape (47%, 6%, and 3%, respectively).

The pattern holds for the regressions in wild canids; the highest correlation coefficients for the humerus are from a regression incorporating centroid size and PCs 1 and 8 ($R^2 = 0.93$, %PE = 19, %SEE = 24). The same is true for the femur, with the best regression using centroid size and PC 1 and 3 ($R^2 = 0.91$, %PE = 22, %SEE = 29). For both the humerus and the femur, PC 1 associates more robust bones with heavier estimates of body mass (Fig. 5). For the humerus, PC 8 links heavier estimates with a taller greater tubercle and a larger medial epicondyle. For the femur, higher scores on PC 3 are associated with a larger lesser

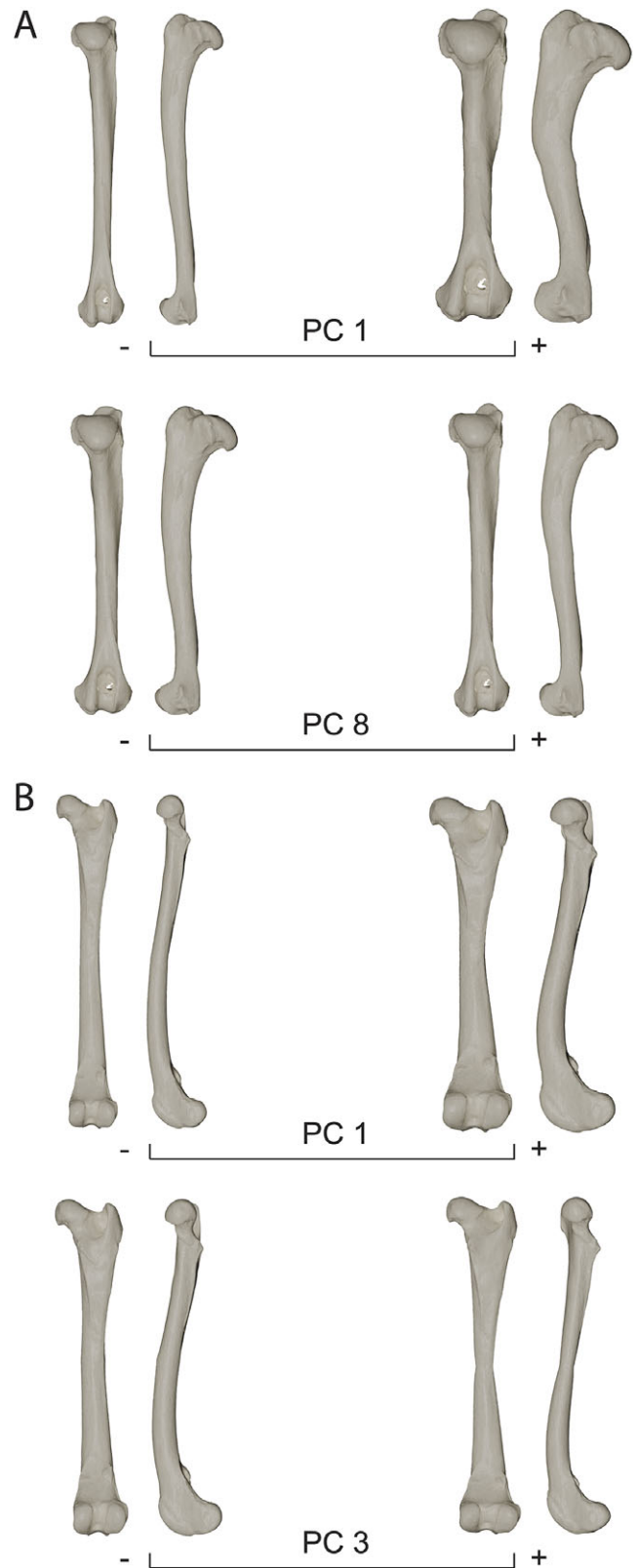


Figure 5. Relevant axes of limb bone variation in wild canids for the humerus (A) and the femur (B). Models show the shape changes associated with the minimum and maximum score for each principal component (PC). PCs are oriented such that heavier individuals are associated with positive scores. For each pair of bones, posterior view is on the left and medial view is on the right.

trochanter and condyles, as well as a wider trochlea. PCs 1 and 8 capture 45% of the variance in the humerus (42% and 3%, respectively), while PCs 1 and 3 capture 42% of the variance in the femur (31% and 11%, respectively). Similar to the results for the linear dimensions, the error levels of even the best estimators are higher in wild canids than in domestic dogs.

Testing Domestic Dog Estimation Equations on Wild Canids

The applicability of body-mass estimation equations derived from domestic dogs to predict the body mass of wild canids was tested by applying the best dog estimation equation for each limb bone to the wild canid dataset, which was rotated into the dog PCA morphospace for this process. In both cases, the best predictive equation was a combination of centroid size and a number of PCs. The initial predictions presented by these equations significantly overestimated body mass in wild canids and had very high error levels for both the humerus (%PE = 70, %SEE = 82) and femur (%PE = 77, %SEE = 85). In comparison, estimations based on the domestic dog linear measurement regressions had only moderately more error than the wild canid based estimations (Table 2).

However, the high degree of error in the morphometric estimations was driven by the relationship between centroid size and body mass. Wild canids have higher centroid sizes across all body masses (Fig. 6A). Because centroid size is a function of the sum of landmark distances from the origin, more gracile bones have comparatively higher centroid sizes. The relative robustness of domestic dogs versus wild canids was assessed using the ratio of epiphysis breadth divided by greatest length, based on the Humeral Epicondylar Index defined by Samuels et al. (2013). This index was measured using distal breadth for the humerus and proximal breadth for the femur, as they had already been measured. In dogs, the average humeral robustness was higher ($\bar{x} = 0.101$, $\sigma = 0.025$) than in wild canids ($\bar{x} = 0.07$, $\sigma = 0.007$). A similar pattern was seen for the femur, with higher mean robustness in dogs ($\bar{x} = 0.092$, $\sigma = 0.015$) than in wild canids ($\bar{x} = 0.069$, $\sigma = 0.005$). This difference in robustness was significant for both bones, as confirmed by *t*-tests (humerus: $p < 0.001$, femur: $p < 0.001$).

This was also visualized by plotting the length of the humerus versus the width of the distal epiphysis (Fig. 6B), which further confirms that domestic dogs are consistently more robust (wider epiphyses for a given length). The effect of this difference in robustness is a consistent overprediction of wild canid body masses when using a domestic dog-derived estimation equation.

Accounting for this effect by subtracting a constant amount (0.48 in humeri, 0.53 in femur, calculated as the mean residual difference between predicted body mass and actual body mass) from all log body-mass predictions significantly improves the error levels in the humerus (%PE = 21, %SEE = 36) and the femur (%PE = 23, %SEE = 41). With this adjustment, the error levels for these regressions are on par with those constructed based on the wild canid dataset. While this adjustment is ad hoc and specific to this dataset, it allows the shape changes observed in domestic dogs to be compared against the patterns in wild canids without the confounding influence of different levels of robustness.

Predicting Mass of Fossil Canids

The body mass of four extinct canids was estimated using a selection of regression equations from each limb bone (Table 3). Because the centroid size is an important part of the best-estimation equations, the domestic dog regressions were applied both alone and in combination with the adjustment applied to wild canids. The robustness of each fossil species was compared with the typical robustness of domestic dogs and gracility of wild canids to determine which estimation equation was a better fit. The same ratios of epiphysis breadth divided by greatest length were calculated for each fossil specimen and assessed using logistic regression (Supplementary Table 6).

For the humerus, *Canis latrans* was placed clearly with the wild canids ($p = 0.85$), while the other species fell in line with the domestic dogs ($p > 0.87$), suggesting that the adjustment for low robustness should be applied for *C. latrans* but not the other species (Fig. 6B). In contrast, for the femur, *Hesperocyon* was weakly placed with the wild canids ($p = 0.68$) instead of the domestic dogs. *Aenocyon dirus* was still categorized as robust ($p > 0.81$) and

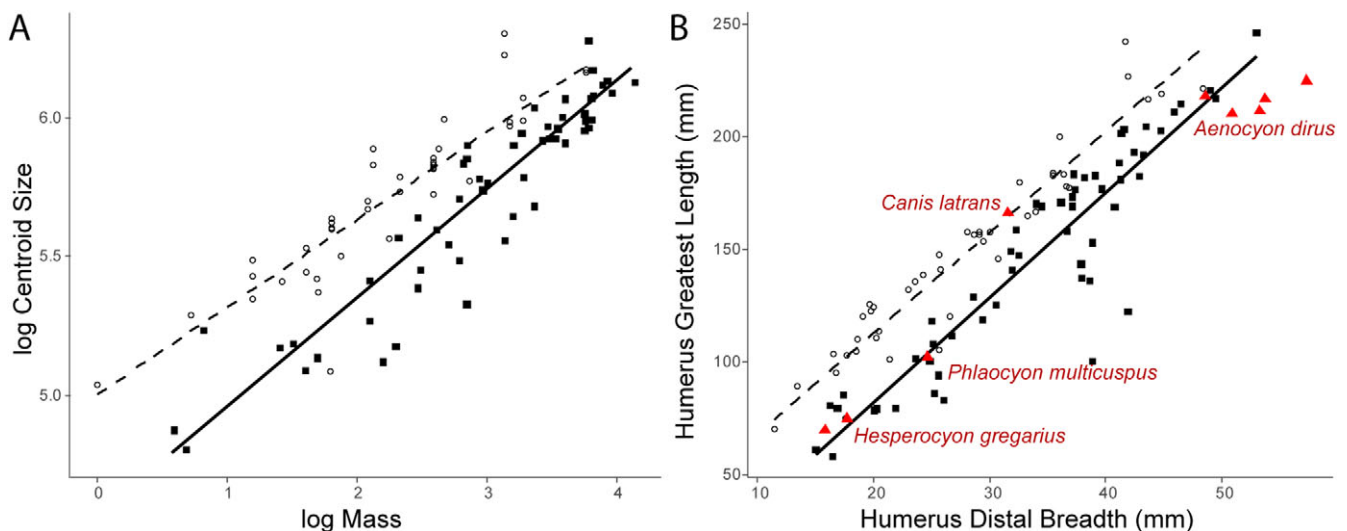


Figure 6. Humerus proportions differ between domestic dogs and wild canids. **A**, Relationship between log body mass and log centroid size. **B**, Relationship between humerus distal breadth and greatest length. The ratio between distal breadth and greatest length was used to assess differences in the degree of robustness among the three groups. Domestic dogs, black squares; wild canids, open circles; fossil canids, red triangles.

Table 3. Estimated body mass for the fossil canids. Estimates are based on 3D limb bone shape and the best domestic dog body-mass estimation equation. For the humerus, this was $\log(\text{centroid}) + \text{PCs } 1, 9$; for the femur, this was $\log(\text{centroid}) + \text{PCs } 1, 3, 7$. Separate estimates of body mass are given with and without the adjustment for decreased robustness in wild canids. Body-mass estimates based on the wild canid shape-estimation equations (humerus: $\log(\text{centroid}) + \text{PCs } 1, 8$; femur: $\log(\text{centroid}) + \text{PCs } 1, 3$) are also included for comparison. The preferred estimate is bolded, see explanation in text. Abbreviation: PC, principal component

Species	Museum no.	Body mass estimate (kg)	Adjusted estimate (kg)	Wild canid estimate (kg)
Humerus				
<i>Canis latrans</i>	FMNH P12402	25.91	16.06	9.46
<i>Aenocyon dirus</i>	FMNH P12389a	68.80	42.66	41.29
<i>Aenocyon dirus</i>	FMNH P12389b	70.18	43.51	41.07
<i>Aenocyon dirus</i>	FMNH P12389c	57.34	35.55	28.96
<i>Aenocyon dirus</i>	FMNH P12389d	65.13	40.39	40.98
<i>Aenocyon dirus</i>	LACM PMS9555	75.67	46.91	48.01
<i>Phlaocyon multicuspus</i>	FMNH P12156	8.18	5.07	3.20
<i>Hesperocyon gregarius</i>	FMNH P12224	2.35	1.46	1.32
<i>Hesperocyon gregarius</i>	FMNH P15428	2.75	1.71	2.03
Femur				
<i>Canis latrans</i>	FMNH PM 3737	26.24	15.45	11.53
<i>Aenocyon dirus</i>	FMNH P12393a	60.17	35.42	31.94
<i>Aenocyon dirus</i>	FMNH P12393b	72.41	42.62	35.52
<i>Hesperocyon gregarius</i>	FMNH P12224	4.10	2.42	1.76

C. latrans was still placed with the wild canids but with lower support ($p = 0.64$).

The preferred predicted body mass for each species is given as follows: 16 kg for *C. latrans*, 67 kg for *A. dirus*, 8 kg for *Phlaocyon multicuspus* and 2.5 kg for *Hesperocyon gregarius*. All estimates of body mass, including predictions based on wild canid 3D shape are available in Table 3.

Discussion

The extreme variation in domestic dogs makes them an ideal model subspecies for testing the effectiveness of new methods of body-mass estimation. Despite being a single subspecies, domestic dogs demonstrate a higher degree of adult skeletal diversity than any other mammal species; with 50-fold variation in body mass (2–100 kg) and 5-fold variation in shoulder height (15–80 cm) (Bannasch et al. 2020). One potential consequence of this wide variation in size and shape is that body-mass estimates in dogs have much higher error levels than would otherwise be expected within a species (about 10% higher than in wolves) (Losey et al. 2015, 2017).

Selective breeding by humans has led to extreme variation across breeds and in particular, many of the standard metrics for body mass (skull size, toothrow length, limb bone dimensions) have been selectively altered, changing the overall relationship with body mass. One notable illustration of this is the prevalence of achondroplasia in dogs. Achondroplasia is a type of short-limbed dwarfism, exemplified by the Jack Russell terrier and corgi, which leads to disproportionately short limbs and thus alters the ratio between long-bone dimensions and body size. Outside of this obvious alteration in proportions, certain breeds have also been bred to have especially long and thin legs (e.g., whippets, saluki, greyhound) or short and stocky limbs (e.g., American Staffordshire terrier, cane corso, mastiff). These changes in shape obscure the

relationship between individual features and body mass. However, this extreme variation also makes domestic dogs an ideal model for evaluating the accuracy of functional morphology-based body-mass estimation methods, which combine multiple aspects of shape, including muscle insertion points, tubercle size, and joint configurations to predict body mass, rather than relying on any single measurement.

Comparison of Regressions

Overall, the geometric morphometric regressions that incorporated both size (as centroid size) and shape (as geometric morphometric PCs) tended to have higher correlation coefficients and higher predictive accuracy than those that were based on size alone (Tables 1, 2). While easier to measure, linear dimensions were consistently worse predictors. This suggests that when geometric morphometrics is an option, it should be the preferred method of estimating body mass.

Of the linear dimensions, percent prediction error (%PE) places proximal humerus depth and proximal femur breadth as the best predictors of body mass in domestic dogs and wild canids. This agrees with Losey et al.'s (2017) previous comparisons of limb element regressions in domestic dogs, although distal humerus breadth was slightly better than proximal depth in their study. While correlation coefficients for linear dimensions were higher in the present study, error levels in dogs were also higher by 2–7% for %PE and 0–14% for %SEE. This could be caused by the differences in the distribution of breeds and sizes between the two datasets. Losey et al.'s dataset contained 43 specimens, from approximately 25 breeds, with a high proportion of Inuit sled dogs. In contrast, the dataset used here includes more breeds in general, as well as more toy and achondroplastic breeds specifically, leading to more overall variation in size and shape.

Unsurprisingly, element lengths were poor estimators of body mass for both the humerus and femur. While easy to measure, element lengths are not often recommended as estimators of body mass, because lengths are not as tightly correlated with body mass as other characteristics, and they often have higher error in comparison to estimates based on cross-sectional or articular dimensions (Egi 2001; Ruff 2003; Losey et al. 2017). Notably, the use of centroid size alone was less precise than humeral or femoral element length in domestic dogs and wild canids. This also suggests that centroid size alone is likely to be a less precise estimator of body mass than it is in combination with shape.

In contrast, the incorporation of just one PC significantly decreased the prediction error of the estimate and increased the correlation coefficient (Tables 1, 2). This indicates that the overall 3D shape of the stylopod is capturing additional information about functional relationships between the skeleton and the body it supports. Thus, despite extreme selective breeding, the shape of the limb bones is still at least partially reflective of functional constraints. To visualize this, the estimation equation parameters from the regression of body mass onto shape were used to warp the mean shape to represent a hypothetical “relatively heavy” limb bone and a hypothetical “relatively light” limb bone (Fig. 7).

Unsurprisingly, the PCs that were most effective at capturing the relationship between mass and shape were related to bone robustness. In large mammals (>100 kg), increases in body mass are partially compensated for by increased bone robustness (Bertram and Biewener 1990). While most smaller mammals have been shown to compensate using postural and behavioral changes (Biewener 1989), the body-mass regressions in this study indicate that there is a correlation between robustness and relative body mass in domestic dogs.

The dominant pattern is that, for a given centroid size, heavier individuals have humeri and femora that are proportionally wide relative to their length and have more pronounced muscle attachments. For the humerus, relatively heavier individuals had a larger greater tubercle, implying a larger muscle attachment site for the supraspinatus and deep pectoral muscle. The supraspinatus is involved in advancing the forelimb and stabilizing the trunk during locomotion, while the pectoralis draws the limb backward to advance the trunk and plays a large role in supporting the trunk. Relatively heavier individuals also had a wider trochlea, which would help stabilize the elbow joints, especially as body mass

increases. Interestingly, in relatively heavier individuals, the insertion point of the deltoid was shifted proximally—which is associated with a shorter moment arm and weaker but faster flexion. This disagrees with previous hypotheses that predict that more distal deltoid tuberosities should be associated with greater maximal body masses (Sorkin 2008). However, it is possible that this relationship differs because the regression used here focuses on relative body mass, not absolute mass. Additionally, only the point of maximum convexity was landmarked, not its distal extent, which may also have a different relationship with mass.

For the femur, relatively heavier individuals were associated with larger muscle attachment sites on the proximal epiphysis, particularly the greater and lesser trochanters. The greater trochanter is the insertion point for the gluteal muscle, which is responsible for the extension of the hip joint. The lesser trochanter is the insertion point for the iliopsoas, which flexes the hip joint to draw the hind limb forward or the trunk backward and assists in stabilization of the vertebral column. Relatively heavier individuals also had a larger lateral supracondylar tuberosity, which is the origin of the lateral head of the gastrocnemius and is responsible for extension of the tarsal joint.

All else being equal, increased body mass requires relatively more robust bones to compensate for the increased stress, as well as relatively larger muscle attachment sites to propel the increased mass. This is especially true for the most proximal muscles of the limb, which insert on the stylopod and provide the bulk of the force required for locomotion.

The great strength of geometric morphometric-based body estimation equations is the ability to synthesize these many subtle aspects of shape in order to construct a more accurate (and more biological) estimate of mass. Previous studies that used centroid size to estimate body mass may have benefited from incorporating a few components of shape into their regressions (Hood 2000; Meloro and O’Higgins 2011; Cassini et al. 2012; Figueirido et al. 2015). Furthermore, the additional effort required by geometric morphometrics is irrelevant in a study that is already using centroid size, as landmarking is a prerequisite for calculating centroid size.

These results also highlight that while Procrustes superimposition mathematically standardizes for size, it does not in any way remove all shape features that are correlated with size, as has been previously shown (Bookstein 1986; Rohlf and Marcus 1993; Meloro and O’Higgins 2011) nor is the influence of size strictly relegated to

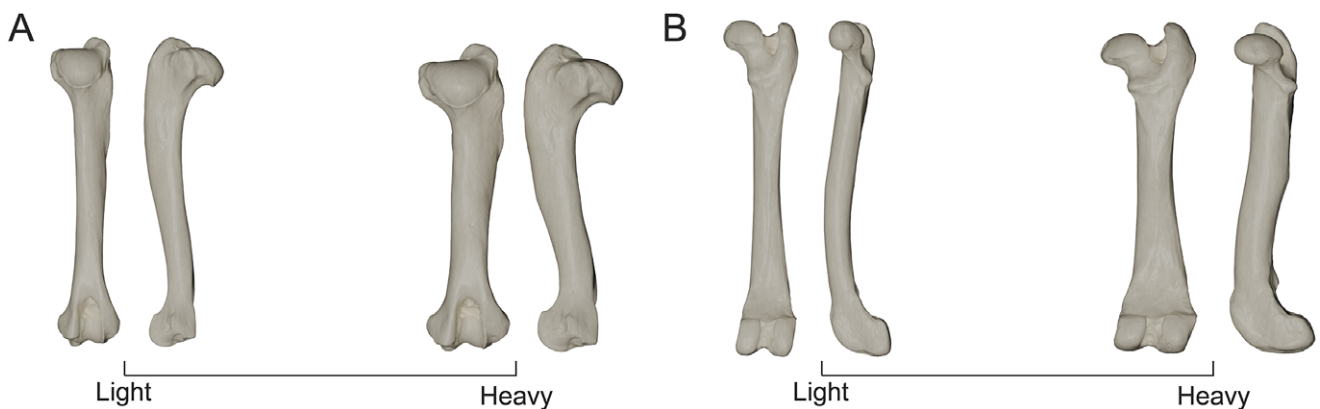


Figure 7. The morphological results of regression of limb bone shape onto body size. Shape models of relatively light and relatively heavy humeri (A) and femora (B) are shown, each generated by warping mean shape along the principal components (PCs) in the body-mass estimation equations. For the humerus, this was $\log(\text{centroid}) + \text{PCs } 1, 9$; for the femur, this was $\log(\text{centroid}) + \text{PCs } 1, 3, 7$. PC scores representing the 10th and 90th quantile of PC variance were used to generate the models. For each pair of bones, posterior view is on the left and medial view is on the right.

only the first PC, as it typically is when the variables are themselves size measurements such as lengths, widths, or volumes. For the humerus, the optimal regression incorporated PCs 1, 2, and 9, while the femur also included three separate PCs. If Procrustes superimposition was truly capable of removing all influence of size, then there would not be any correlation worth incorporating in the regression. While Procrustes standardizes for overall mathematical size, it does not remove the allometric relationship of size to shape.

When they want truly size-free shape variables, some authors have used allometry-free shape coordinates, whereby some measure of size is regressed out of geometric morphometric data in order to analyze an aspect of shape without any influence of “size.” There is the tendency to use centroid size rather than body mass when calculating allometry-free coordinates (Bookstein 1989, 1996). While centroid size is one way to measure size, and is thus a valid way to calculate allometry, it is not equivalent to body mass or body length and captures a very different allometric relationship. These results show, foremost, that centroid size does not always have the strongest relationship with body mass. Second, these results emphasize that even once centroid size has been taken into account, there still remain aspects of size allometry included in the shape components. If the goal is to remove overall body size, then allometry-free coordinates would be better calculated with body mass or body length when it is available and not a proxy (although I recognize that independent measures of body size are not always available). Finally, centroid size is highly variable and entirely dependent on the bones used and the choice of landmark position. Allometric scaling relationships vary between bones (Garcia and Dasilva 2006), which means that the choice of bone will impact the calculation of allometry. Similarly, it is possible that different landmarking schemes could return different size orderings. Certain shapes, like long thin projections, have the potential to unduly skew centroid size (Bookstein 1991). Caution should be taken when using centroid size to calculate allometry-free coordinates if the goal is actually to remove the influence of body mass or body length.

Disadvantages to 3D Morphometric Body-Mass Estimation

While geometric morphometrics can provide estimates of body mass that are more accurate, it should be made clear that estimating body mass using 3D shape does have its drawbacks. This method is significantly more time-consuming than estimations made using linear measurements and produces regression equations that are sample dependent. Geometric morphometrics also requires more intact fossil specimens, which can heavily restrict sample sizes, although landmarks could be restricted to a single epiphysis to allow the inclusion of incomplete specimens.

Using Domestic Dog Regressions to Predict Body Size in Wild Canids

The initial application of domestic dog body-mass estimation regressions on wild canids was largely unsuccessful due to the consistently higher centroid sizes in wild canids. However, once this relationship was corrected for, the predictive accuracy was as high as the regressions based on wild canids alone. This suggests that the limb bone allometry of domestic dogs and wild canids is similar enough, despite the large degree of selective breeding in dogs, that regressions based on domestic dogs can reasonably be applied to predicting the body mass of wild canids successfully, and potentially fossil canids as well.

This congruence between dogs and wild canids allows the incredible variation in domestic dogs, as well as the large base of existing

dog literature, to be leveraged toward a better understanding of the biology of both living and extinct canid species.

That said, there are differences between domestic dogs and their wild ancestors. This study found a striking difference in the patterns of limb bone centroid size between domestic dogs and wild canids. The wild canids had consistently higher centroid sizes at all body masses as a result of longer and more gracile limb bones. This variation in the relationship between centroid size and body mass should serve as a further caution against using centroid size alone for body-mass estimation.

Future studies could investigate the difference in centroid size between wild and domestic canids and explore the link between this pattern and domestication syndrome (Wilkins et al. 2014).

Fossil Estimates

Body mass was predicted for four fossil taxa using the best regressions for each limb bone in domestic dogs and wild canids. Each of the four regressions utilized a combination of log centroid size and a few PCs of shape. For the domestic dog regressions, it is necessary to consider whether the centroid size correction applied to wild canids should also be applied to fossil ones. If the robustness of domestic dog limb bones is a result of domestication, then all fossil canids would need to be corrected like wild canids. However, if the gracility of modern wild canids is an adaptation for cursoriality specific to the most recent radiation of canids (Figueirido et al. 2015), then we would not expect the oldest fossil canids to share these proportions, and it may be more accurate to group the more robust fossil canids with the domestic dogs. Given the lack of a straightforward answer, both estimated mass ranges are presented for the examined species in Table 3, and the preferred estimate was chosen based on the degree of morphological robustness (Fig. 6).

The predicted body mass for *Canis latrans orcutti*, an extinct subspecies of coyote known best from the late Pleistocene Rancho La Brea site, was 16 kg with the adjusted regression. *Canis latrans* was the most gracile of the fossils investigated, with similar proportions to the wild canids, including the modern representative of this species: the coyote. Given this, the adjusted regression is the most reasonable choice for this species. This would place the estimate of 16 kg within the range of modern coyote body mass: 7–20 kg (Bekoff 1977).

The Pleistocene dire wolf, *Aenocyon dirus*, had robust limb bone proportions more similar to those of domestic dogs than wild canids, supporting the use of the unadjusted domestic dog regression. This regression gives an estimated average body mass of 67 kg, which is very similar to previous estimates of 60–68 kg (Anyonge and Roman 2006; Figueirido et al. 2015).

Phlaocyon multicuspus, a hypocarnivorous canid from the Miocene, also had robust limb proportions, which suggests that the unadjusted regression would be the best fit, leading to an estimated body mass of 8 kg. No previous estimates of body mass exist for this species, so for comparison purposes, body mass for this species was estimated using cranial measurements and preexisting estimation equations for Canidae (Van Valkenburgh 1990; Wang et al. 1999). Estimating body mass from skull length gave a predicted mass of 4.8 kg, which is lower than the estimate from humerus shape. This is likely driven by differences in head–body proportions between extant canids and the extinct borophagines. The degree of error for cranial measurements is often higher than those based on dental characteristics; however, the preferred lower first molar has not been preserved for this species. Given the generally higher accuracy of postcranial estimations, *P. multicuspus* was likely more massive

than skull size alone would suggest. However, it is also worth noting that the adjusted estimate of body mass (5 kg) is very similar to the cranial estimate of body mass.

For *Hesperocyon gregarius*, an extinct fox-sized canid from the Oligocene, limb proportions did not fall clearly with either domestic dogs or wild canids. The humerus was more robust, in line with domestic dogs, while the femur was comparatively gracile, leading to an average estimate of 2.5 kg. This estimate falls between the previous estimates of 3.6 kg made by Figueirido et al. (2015) based on the centroid of the elbow and the 2 kg estimate presented by Finarelli and Flynn (2006) based on dental measurements. Both the estimates based on wild canid 3D shape (1.7 kg) and the adjusted domestic dog estimate (1.9 kg) are close to the Finarelli and Flynn (2006) estimate of 2 kg.

Conclusions

1. When reasonable, 3D morphometrics can provide more accurate body-mass estimations than estimates based on linear measurements. This comes at a trade-off to the increased time required for geometric morphometric analyses.
2. Body-mass estimates based on centroid size are much less accurate than standard linear measurements, while still requiring the same time investment as a full 3D estimation equation.
3. Wild canids are consistently more gracile than domestic dogs. This means domestic dogs are a poor comparative model for estimating body mass in wild canids unless adjustments are applied to account for the differences in robustness.
4. Two of the four fossil canids here had robustness indices that placed them closer in proportion to domestic dogs than modern wild canids, suggesting that domestic dogs may be useful as a proxy for studying fossil canids.
5. New estimates of body mass are presented for *Canis latrans*, *Aenocyon dirus*, and *Hesperocyon gregarius*, as well as the first cranial and postcranial estimates of body mass for *Phlaocyon multicuspus*.

Acknowledgments. I would like to thank P. D. Polly (Indiana University, Bloomington, Indiana) for his advice and assistance in preparing this paper. Also, thanks to R. Baumgardner, J. Lattimer, and the University of Missouri at Columbia Veterinary Health Center for allowing me access to their database of dog CT scans; to A. Ferguson and B. Simpson at the Field Museum; and to D. Lunde, J. Ososky, and T. Hsu at the National Museum of Natural History for their aid in accessing their respective collections.

Competing Interests. The author declares no conflicts of interest.

Data Availability Statement. Data available from the Dryad Digital Repository: <https://doi.org/10.5061/dryad.tx95x6b78>. Source code and additional data available from Zenodo: <https://doi.org/10.5281/zenodo.14361342> and <https://doi.org/10.5281/zenodo.14361346>.

Literature Cited

Adams, D. C., M. L. Collyer, A. Kaliontzopoulou, and E. K. Baken. 2021. Geomorph: software for geometric morphometric analyses. R package version 4.0. <https://cran.r-project.org/package=geomorph>, accessed 27 April 2024.

[AKC] American Kennel Club. 2023. Home page. <https://www.akc.org>, accessed 31 January 2023.

Andersson, K. 2004. Predicting carnivoran body mass from a weight-bearing joint. *Journal of Zoology* 262:161–172.

Anyonge, W. 1993. Body mass in large extant and extinct carnivores. *Journal of Zoology* 231:339–350.

Anyonge, W., and C. Roman. 2006. New body mass estimates for *Canis dirus*, the extinct Pleistocene dire wolf. *Journal of Vertebrate Paleontology* 26: 209–212.

Bailey, R. C., and J. Byrnes. 1990. A new, old method for assessing measurement error in both univariate and multivariate morphometric studies. *Systematic Zoology* 39:124.

Bannasch, D. L., C. F. Baes, and T. Leeb. 2020. Genetic variants affecting skeletal morphology in domestic dogs. *Trends in Genetics* 36:598–609.

Bekoff, M. 1977. *Canis latrans*. *Mammalian Species* 79:1–9.

Bertram, J. E. A., and A. A. Biewener. 1990. Differential scaling of the long bones in the terrestrial Carnivora and other mammals. *Journal of Morphology* 204:157–169.

Biewener, A. 1989. Scaling body support in mammals: limb posture and muscle mechanics. *Science* 245:45–48.

Bookstein, F. L. 1986. Size and shape spaces for landmark data in two dimensions. *Statistical Science* 1:181–222.

Bookstein, F. L. 1989. “Size and shape”: a comment on semantics. *Systematic Zoology* 38:173–180.

Bookstein, F. L. 1991. *Morphometric tools for landmark data*. Cambridge University Press, New York.

Bookstein, F. L. 1996. Combining the tools of geometric morphometrics. Pp. 131–151 in L. F. Marcus, M. Corti, A. Loy, G. J. P. Naylor, and D. E. Slice, eds. *Advances in morphometrics*. Springer US, Boston.

Carbone, C., G. M. Mace, S. C. Roberts, and D. W. Macdonald. 1999. Energetic constraints on the diet of terrestrial carnivores. *Nature* 402:286–288.

Cassini, G. H., S. F. Vizcaíno, and M. S. Bargo. 2012. Body mass estimation in Early Miocene native South American ungulates: a predictive equation based on 3D landmarks. *Journal of Zoology* 287:53–64.

Egi, N. 2001. Body mass estimates in extinct mammals from limb bone dimensions: the case of North American hyaenodontids. *Palaeontology* 44:497–528.

Eisenberg, J. F. 1981. *The mammalian radiations: an analysis of trends in evolution, adaptation, and behavior*. University of Chicago Press, Chicago.

Evans, H. E., and M. E. Miller. 1993. *Miller’s anatomy of the dog*. Saunders, Philadelphia.

Fabre, A.-C., A. Goswami, S. Peigné, and R. Cornette. 2014. Morphological integration in the forelimb of musteloid carnivorans. *Journal of Anatomy* 225:19–30.

Fedorov, A., R. Beichel, J. Kalpathy-Cramer, J. Finet, J.-C. Fillion-Robin, S. Pujol, C. Bauer, et al. 2012. 3D Slicer as an image computing platform for the Quantitative Imaging Network. *Magnetic Resonance Imaging* 30:1323–1341.

Figueirido, B., A. Martín-Serra, Z. J. Tseng, and C. M. Janis. 2015. Habitat changes and changing predatory habits in North American fossil canids. *Nature Communications* 6:7976.

Finarelli, J. A., and J. J. Flynn. 2006. Ancestral state reconstruction of body size in the Caniformia (Carnivora, Mammalia): the effects of incorporating data from the fossil record. *Systematic Biology* 55:301–313.

Garcia, G., and J. Dasilva. 2006. Interspecific allometry of bone dimensions: a review of the theoretical models. *Physic of Life Reviews* 3:188–209.

Hebbali, A. 2024. olsrr: tools for building OLS regression models. R package version 0.6.0. <https://CRAN.R-project.org/package=olsrr>, accessed 27 April 2024.

Hood, C. 2000. Geometric morphometric approaches to the study of sexual size dimorphism in mammals. *Hystrix, the Italian Journal of Mammalogy* 11. <https://doi.org/10.4404/hystrix-11.1-4137>.

Losey, R. J., B. Osipov, R. Sivakumaran, T. Nomokonova, E. V. Kovychev, and N. G. Diatchina. 2015. Estimating body mass in dogs and wolves using cranial and mandibular dimensions: application to Siberian canids. *International Journal of Osteoarchaeology* 25:946–959.

Losey, R. J., K. McLachlin, T. Nomokonova, K. Latham, and L. Harrington. 2017. Body mass estimates in dogs and North American gray wolves using limb element dimensions. *International Journal of Osteoarchaeology* 27: 180–191.

MacNulty, D. R., D. W. Smith, L. D. Mech, and L. E. Eberly. 2009. Body size and predatory performance in wolves: is bigger better? *Journal of Animal Ecology* 78:532–539.

Martín-Serra, A., B. Figueirido, and P. Palmqvist. 2014a. A three-dimensional analysis of the morphological evolution and locomotor behaviour of the carnivoran hind limb. *BMC Evolutionary Biology* 14:129.

- Martín-Serra, A., B. Figueirido, and P. Palmqvist.** 2014b. A three-dimensional analysis of morphological evolution and locomotor performance of the carnivoran forelimb. *PLoS ONE* **9**:e85574.
- Mazerolle, M. J.** 2023. AICcmodavg: model selection and multimodel inference based on (Q)AIC(c). R package version 2.3-3. <https://cran.r-project.org/package=AICcmodavg>, accessed 27 April 2024.
- McNab, B. K.** 1990. The physiological significance of body size. Pp. 11–23 in J. Damuth and B. J. MacFadden, eds. *Body size in mammalian paleobiology: estimation and biological implications*. Cambridge University Press, Cambridge.
- Meloro, C., and P. O'Higgins.** 2011. Ecological adaptations of mandibular form in fissiped Carnivora. *Journal of Mammalian Evolution* **18**:185–200.
- Muñoz-Muñoz, F., and D. Perpiñán.** 2010. Measurement error in morphometric studies: comparison between manual and computerized methods. *Annales Zoologici Fennici* **47**:46–56.
- R Core Team.** 2018. *R: a language and environment for statistical computing*. R Foundation for Statistical Computing, Vienna, Austria.
- Rohlf, F. J., and L. F. Marcus.** 1993. A revolution in morphometrics. *Trends in Ecology and Evolution* **8**:129–132.
- Rohlf, F. J., and D. Slice.** 1990. Extensions of the Procrustes method for the optimal superimposition of landmarks. *Systematic Zoology* **39**:40.
- Rovinsky, D. S., A. R. Evans, D. G. Martin, and J. W. Adams.** 2020. Did the thylacine violate the costs of carnivory? Body mass and sexual dimorphism of an iconic Australian marsupial. *Proceedings of the Royal Society B* **287**:20201537.
- Ruff, C. B.** 2003. Long bone articular and diaphyseal structure in Old World monkeys and apes. II: Estimation of body mass. *American Journal of Physical Anthropology* **120**:16–37.
- Samuels, J. X., J. A. Meachen, and S. A. Sakai.** 2013. Postcranial morphology and the locomotor habits of living and extinct carnivorans. *Journal of Morphology* **274**:121–146.
- Sorkin, B.** 2008. A biomechanical constraint on body mass in terrestrial mammalian predators. *Lethaia* **41**:333–347.
- Van Valkenburgh, B.** 1990. Skeletal and dental predictors of body mass in carnivores. Pp. 181–205 in J. D. Damuth and B. J. MacFadden, eds. *Body size in mammalian paleobiology estimation and biological implications*. Cambridge University Press, Cambridge.
- Von den Driesch, A.** 1976. *A guide to the measurement of animal bones from archaeological sites*, Vol. 1. Peabody Museum Press, Cambridge, Mass.
- Wang, X., R. H. Tedford, and B. E. Taylor.** 1999. Phylogenetic systematics of the Borophaginae (Carnivora: Canidae). *Bulletin of the American Museum of Natural History* **243**:391.
- Wilkins, A. S., R. W. Wrangham, and W. T. Fitch.** 2014. The “domestication syndrome” in mammals: a unified explanation based on neural crest cell behavior and genetics. *Genetics* **197**:795–808.
- Yezerinac, S. M., S. C. Loughheed, and P. Handford.** 1992. Measurement error and morphometric studies: statistical power and observer experience. *Systematic Biology* **41**:471–482.